Supplemental Materials

Molecular Biology of the Cell

Cencer *et al*.

SUPPLEMENTAL INFORMATION

“Loss of intermicrovillar adhesion factor CDHR2 impairs basolateral junctional complexes in transporting epithelia.”

By Caroline S. Cencer, Kianna L. Robinson, and Matthew J. Tyska

Supplemental Video

Video S1, related to Figure 4.

Supplemental Figures

Figure S1, related to Figure 1. Generation and validation of CDHR2 KO CACO-2_{BBE} cells.

Figure S2, related to Figure 2. Further characterization of the CDHR2 KO phenotype.

Figure S3, related to Figures 2, 3, and 4. CDHR2 KO CL4 cells exhibit reduced levels of CDHR5 and ZO-1, which are rescued upon expression of HALO-tagged CDHR2. ZO-1 and villin are depleted in the CDHR2 KO mouse small intestine (duodenum). Collective migration during wound healing is defective in CDHR2 KO CL4 monolayers.

Fig. S1

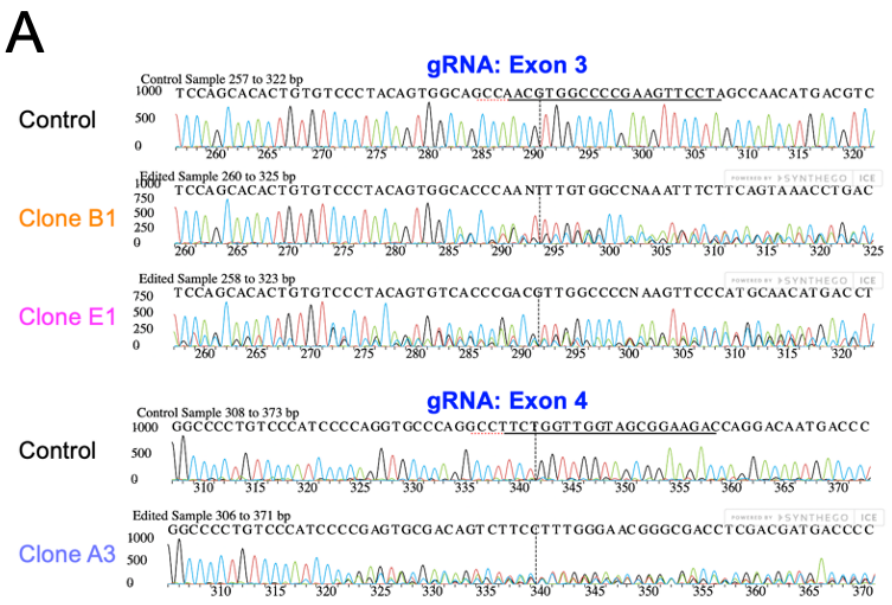

KO Clone	gRNA sequence	PAM	INDEL %	MODEL FIT (R^2)	KNOCKOUT-SCORE
B1	TAGGAACTTCGGGGCCACGT	TGG	91	0.91	31
E1	TAGGAACTTCGGGGCCACGT	TGG	85	0.85	85
A3	GTCTTCCGCTACCAACCAGA	AGG	93	0.93	93

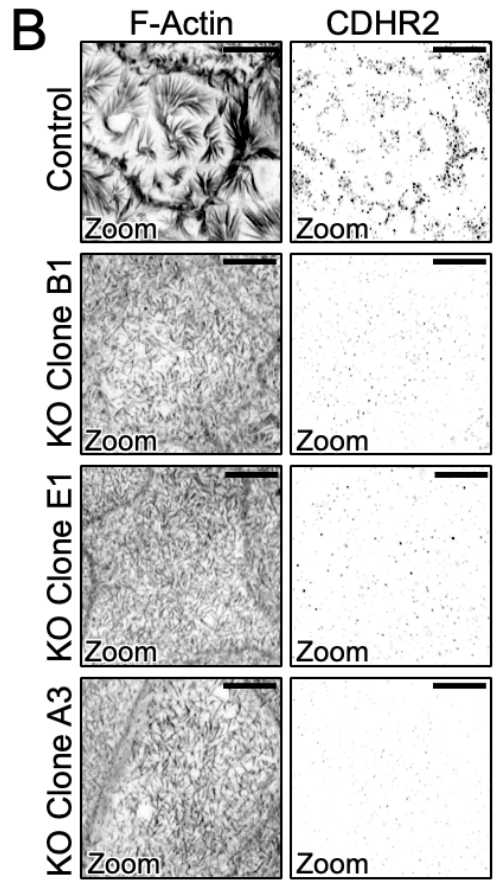

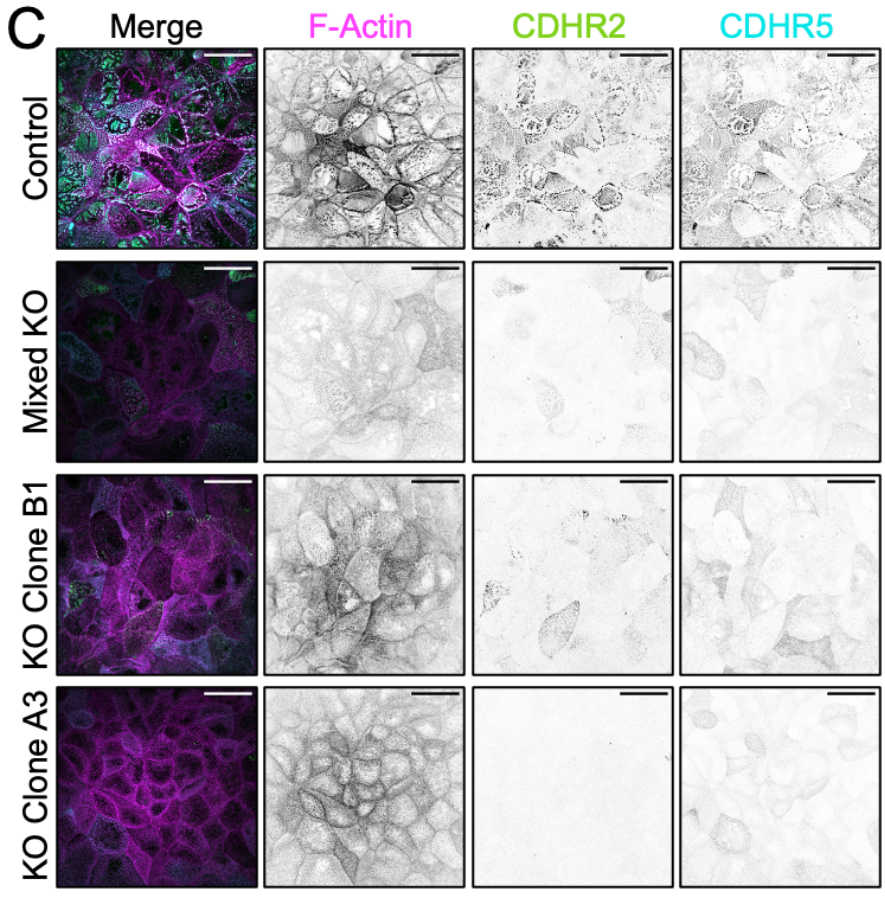

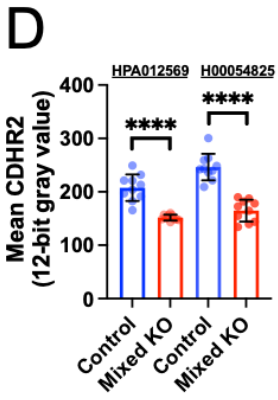

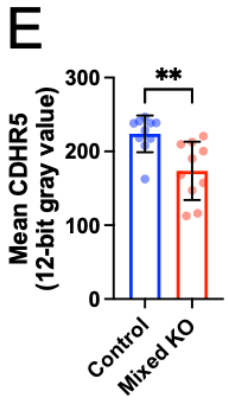

Figure S1, related to Figure 1. Generation and validation of CDHR2 KO CACO-2$_{BBE}$ cells. (A) Genomic DNA was extracted from selected KO clonal populations and PCR was used to generate two regions spanning exons 3 and 4 of CDHR2. Trace files of each clone and the control cells were analyzed with the Synthego Inference of CRISPR Edits (ICE) tool (Conant et al., 2022). (B) Laser scanning confocal MaxIP images of Control, CDHR2 KO Clone “B1”, “E1”, and “A3” stained for F-Actin and CDHR2 as labeled showing lack of microvillar clustering in the KO cells. (C) Yokogawa W1 spinning disk MaxIP images of Control, mixed KO (pre-clonal isolation), and KO clones stained for F-Actin (magenta), CDHR2 (green), and CDHR5 (cyan). (D) Mean CDHR2 intensities of Control vs. CDHR2 mixed KO using two different CDHR2 antibodies, as marked. (E) Mean CDHR5 intensities of Control vs. CDHR2 mixed KO. n = 10 60X fields per condition. Unpaired t-test; ***p≤0.0005, **p<0.005. Error bars represent mean ± SD. Scale bars: 5 μm (B), 30 μm (C).

Fig. S2

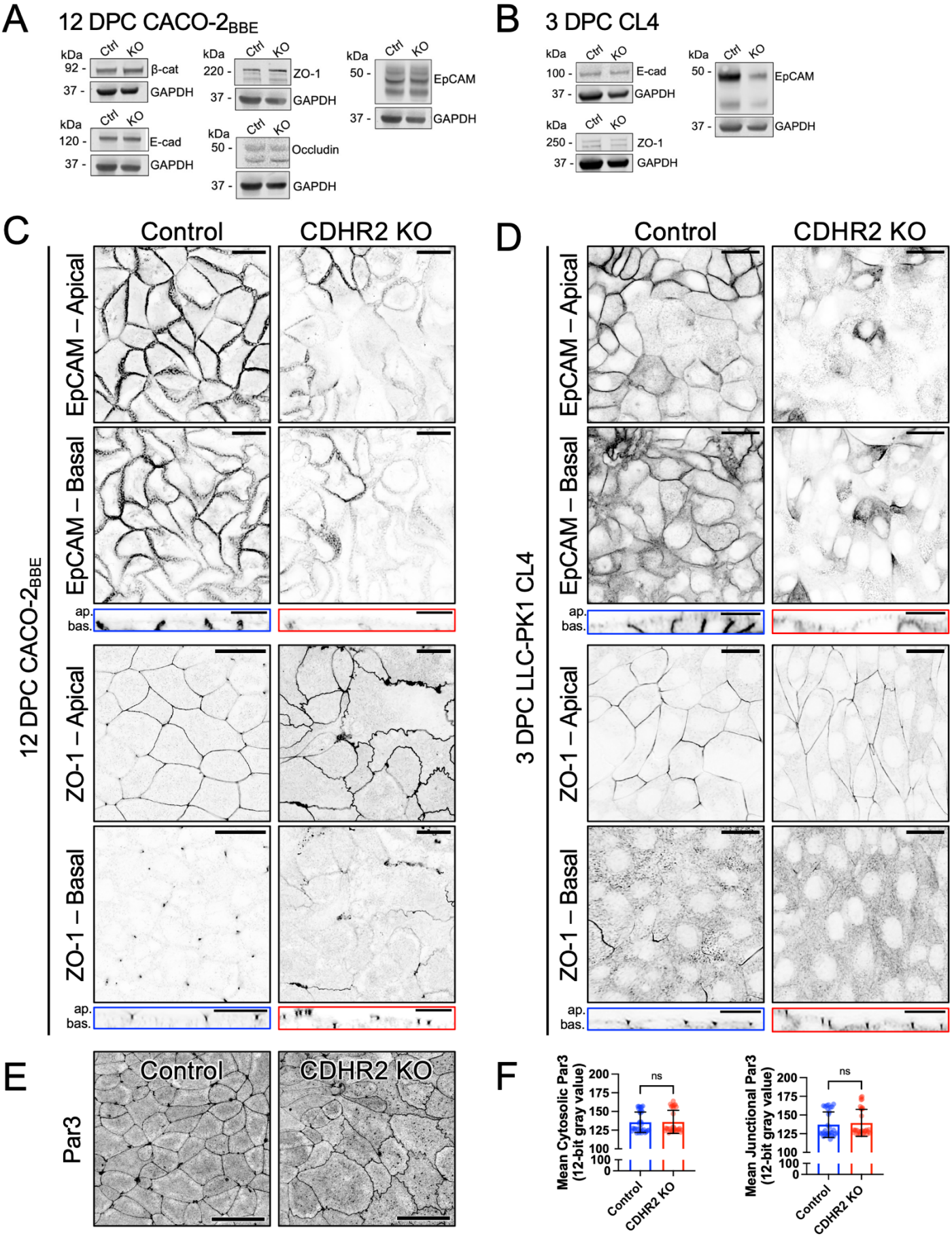
A
12 DPC CACO-2BBE
kDa
Ctrl
KO
92 -
β-cat
37 -
GAPDH
220 -
ZO-1
120 -
E-cad
50 -
Occludin
EpCAM
B
3 DPC CL4
100 -
250 -
C
Control
CDHR2 KO
EpCAM – Apical
EpCAM – Basal
ap.
bas.
ZO-1 – Apical
ZO-1 – Basal
D
3 DPC LLC-PK1 CL4
E
Par3
F
Mean Cytosolic Par3 (12-bit gray value)
Mean Junctional Par3 (12-bit gray value)
ns
200
175
150
125
100
0

Figure S2, related to Figure 2. Further characterization of the CDHR2 KO phenotype. (A) Western blots of whole cell lysates from12 DPC Control and CDHR2 KO CACO-2_{BBE} cells probed with antibodies directed against the indicated junctional components. (B) Western blots of whole cell lysates from 3 DPC Control and CDHR2 KO CL4 cells probed with antibodies directed against the indicated junctional components. (C) Single confocal sections of apical and basal planes from Control and CDHR2 KO CACO-2_{BBE} cells stained for EpCAM and ZO-1 (top and bottom, respectively) at 12 DPC. Lateral (i.e. vertical) sections from Control (blue) and CDHR2 KO (red) confocal volumes are shown below each case. (D) Single confocal sections of apical and basal planes from Control and CDHR2 KO CL4 cells stained for EpCAM and ZO-1 (top and bottom, respectively) at 3 DPC. Lateral (i.e. vertical) sections from Control (blue) and CDHR2 KO (red) confocal volumes are shown below each case. (E) Inverted single channel confocal images of Par3 staining in 12 DPC Control and CDHR2 KO CACO-2_{BBE} cells. (F) Mean cytosolic (left) and junctional (right) Par3 intensities of Control vs. CDHR2 KO CACO-2_{BBE} cells, measured from three replicates, consisting of 10 60X image fields per replicate. Unpaired t-test; ***$p \leq 0.0005$, **$p < 0.005$. Error bars represent mean ± SD. Scale bars: 5 μm (B), 30 μm (C).

Fig. S3

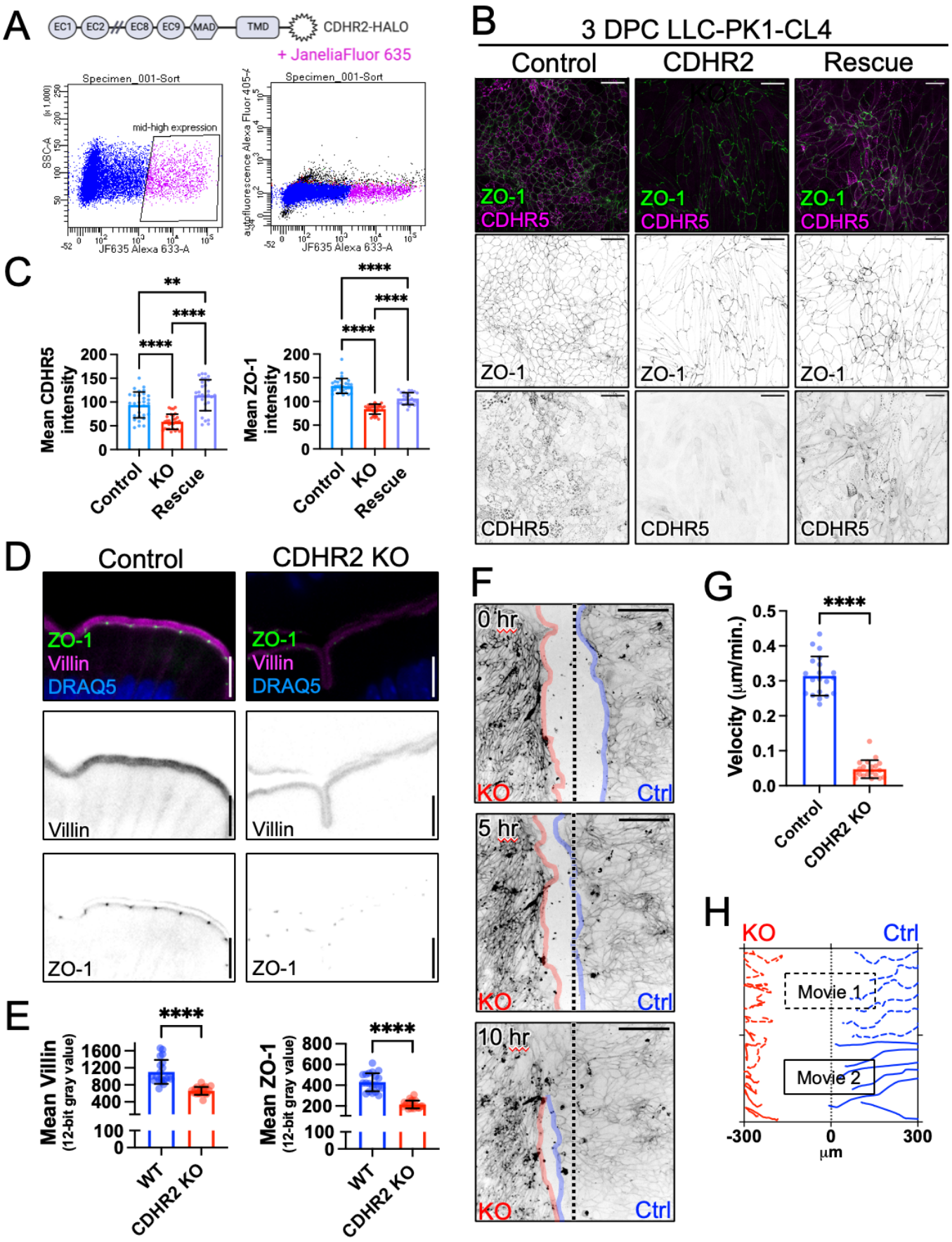
A
EC1
EC2
EC8
EC9
MAD
TMD
CDHR2-HALO
+ JaneliaFluor 635
Specimen_001-Sort
mid-high expression
SSC-A
JF635 Alexa 633-A
Specimen_001-Sort
autofluorescence Alexa Fluor 405-A
JF635 Alexa 633-A
B
3 DPC LLC-PK1-CL4
Control
CDHR2
Rescue
ZO-1
CDHR5
ZO-1
CDHR5
C
Mean CDHR5 intensity
Mean ZO-1 intensity
Control
KO
Rescue
D
Control
CDHR2 KO
ZO-1
Villin
DRAQ5
Villin
ZO-1
E
Mean Villin (12-bit gray value)
Mean ZO-1 (12-bit gray value)
WT
CDHR2 KO
F
0 hr
5 hr
10 hr
KO
Ctrl
G
Velocity (μm/min.)
Control
CDHR2 KO
H
KO
Ctrl
Movie 1
Movie 2
μm

Figure S3, related to Figures 2, 3, and 4. CDHR2 KO CL4 cells exhibit reduced levels of CDHR5 and ZO-1, which are rescued upon expression of HALO-tagged CDHR2. (A) Diagram of the C-terminally tagged CDHR2-HALO construct used for rescue. “Rescue” cells were transfected, stably selected for CDHR2-HALO, and FACS sorting was then used to capture ‘medium-high’ expressing cells based on fluorescence of the JF635 HALO ligand. (B) Confocal MaxIPs of 3 DPC Control, CDHR2 KO, and CDHR2-HALO rescue CL4 cells stained for ZO-1 (green) and CDHR5 (magenta). (C) Mean CDHR5 and ZO-1 intensities for the three cell conditions. n = 30 imaged 40X fields per condition from 3 independent staining experiments. **p = 0.0095, ****p ≤ 0.0001 Ordinary one-way ANOVA with post-hoc multiple comparisons test. Error bars represent mean ± SD. Scale bars in B are 40 μm. **ZO-1 and villin are depleted in the CDHR2 KO mouse small intestine (duodenum).** (D) Confocal MaxIPs of 10 μm paraffin sections stained for ZO-1 (green), villin (magenta), and DRAQ-5 (blue) from wildtype Control and CDRH2 KO mice. Top row shows three-channel merged; inverted single channel images are shown below each merge. LUTs are matched/scaled to Control images. (E) Thresholded mean ZO-1 and villin intensity measurements from two age matched pairs of Control and CDHR2 KO littermates, with 20 measured villi per condition. ****p ≤ 0.0001 unpaired t-test. Error bars represent mean ± SD. Scale bars: 40 μm (A-B), 10 μm (Zooms). **Collective migration during wound healing is defective in CDHR2 KO CL4 monolayers.** (F) Mixed Ibidi chamber wound healing assay with CDHR2 KO (left) and Control CL4 cells (right) labeled with CellBrite650 and imaged over 10 hours following barrier removal. (G) Leading edge velocities of n = 20 Control and KO CL4 cell traces from two timelapse replicates. Unpaired t-test; ****p<0.005. Error bars represent mean ± SD. (H) Trajectories of individual cells tracked in two timelapse replicates (Movie 1 shown in F). Scale bars: 60 μm (C), 200 μm (E).